Combined Effects of the Polarity of Terminal Groups and the Direction of Ester Linkages on Crystalline and Mesophase Structures of Biphenyl Esters with a Cyano or a Methoxy Group

Mutsuko Oki and Kayako Hori*

Department of Chemistry, Ochanomizu University, Otsuka, Bunkyo-ku, Tokyo 112

(Received June 5, 1997)

The crystal structures have been determined for 4′-octyloxybiphenyl-4-yl 4-cyanobenzoate (abbr. OCO-CN) and 4-methoxyphenyl 4′-octyloxybiphenyl-4-carboxylate (abbr. COO-OCH_3) with the identical phase sequence of crystal 1 (CR1)-crystal 2 (CR2)-monolayered smectic A (S_{A1})-nematic (N)-isotropic. It is found that the combination of two factors, (1) opposite polarity of the terminal groups (electron-donating OCH_3 or -accepting CN) and (2) opposite direction of the central ester linkages, results in almost the same structures of CR1. They are composed of bilayers, in which the polar groups face each other. Methoxy groups are in van der Waals contact, while cyano groups have an unfavorable head-to-head arrangement. It is interpreted that this arrangement of CN groups is responsible for the large molecular rearrangements at the CR1–CR2 transition.

When a mesogenic molecule carries two or more polar groups, the intramolecular interaction of the polar groups has a significant influence on the mesophase behavior.[1] The following pairs of compounds show that mesophase sequences are determined by two factors: (1) the nature of the terminal polar group and (2) the direction of the central ester linkage. Namely, whether the terminal polar group is electron-donating or -accepting results in an alternate mesophase sequence (crystal -smectic A (S_A)-nematic (N)-isotropic or crystal-N-iso.) according to the direction of the central ester linkage.[2]

4′-Octyloxybiphenyl-4-yl 4-Y-benzoates (Y = methoxy or cyano)

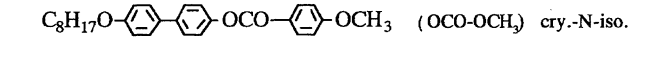

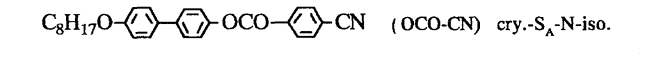

4-Y-phenyl 4′-octyloxybiphenyl-4-carboxylate (Y=methoxy or cyano)

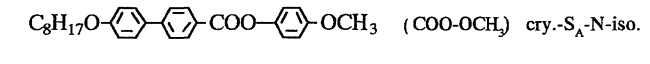

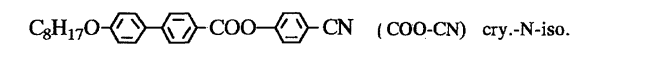

It was also reported that OCO-CN has the S_A phase comprising monolayers (S_{A1}).[3] This is peculiar to this compound and its lower homologues, because cyano compounds including its higher homologues[3] usually have the S_A phase comprising interdigitated bilayers (S_{Ad}) due to the strong dipole moment of the CN group.[4,5]

To identify the intermolecular interaction controlling mesophase behavior, we have determined crystal structures. For two isomeric series of cyano esters, for example, 4-cyanophenyl 4-*n*-alkoxybenzoates and 4-*n*-alkoxyphenyl 4-cyanobenzoates, in which the direction of the ester linkage is opposite each other with respect to the cyano group, a good correlation was found between the crystal structures and the mesophase sequences.[6] Furthermore, the crystal structure of OCO-OCH_3 has already been reported to have an 'imbricated' structure:[7] i.e., a half-and-half overlapping of molecules, being closely related to the phase sequence of cry.-N-iso. This paper describes the crystal structures of OCO-CN and COO-OCH_3 and structural changes from the crystals to the S_A phase investigated by differential scanning calorimetry (DSC) and powder X-ray diffraction measurements. As for COO-CN, the fourth compound, we have not succeeded in determining the crystal structure, because of the very poor crystallinity.

Experimental

Compounds. Both compounds were synthesized in a conventional way.[2]

Apparatus. The thermal behavior was studied using a Seiko SSC22C calorimeter. Powder X-ray diffraction patterns were obtained on a Rigaku PMG-RA CN2155R5 goniometer (λ = 1.5418 Å) equipped with a temperature controller (accuracy of ±0.1 K).

X-Ray Crystal Structure Analysis. Single crystals were obtained by slow evaporation from an acetone-water solution for OCO-CN and an ethyl acetate–ethanol solution for COO-OCH_3 at room temperature. Cell-parameter measurements and reflection data collection were carried out on an AFC-7R four-circle diffractometer using Cu $K\alpha$ radiation monochromated by graphite (λ = 1.54184 Å) at room temperature. The ω mode was used at a scan rate of 2° min^{-1} up to 2θ = 110° for OCO-CN and with a scan rate of 4° min^{-1} up to 2θ = 120° for COO-OCH_3. Three standard reflections were measured after every 150 reflections. No

significant variations were observed. All of the reflection data were corrected for Lorentz and polarization factors. The detailed experimental conditions, crystal data, and final results of the refinements are summarized in Table 1. In both crystals, the ESD's of the cell lengths for *a* and *c* are rather high, because there were only reflections with small indices of *h* and *l* in the appropriate 2θ range due to the extremely long *b* axis and, moreover, the systematic absences on *h* and *l*.

The structures were solved by applying the programs MITHRIL84[8] and SHELXS86[9] for OCO-CN and COO-OCH_3, respectively, and refined by full-matrix least-squares on F^2 by using SHELXL93.[10] All of the non-hydrogen atoms were refined anisotropically. The hydrogen-atom positions, calculated geometrically (C–H distances; 0.96 for primary, 0.97 for secondary, and 0.93 Å for aromatic), were included in structure-factor calculations, but not refined. The atomic scattering factors were taken from International Tables for Crystallography.[11] The final atomic coordinates are given in Tables 2 and 3.[12]

Results and Discussion

Molecular Structures. Figure 1 shows ORTEP[13] drawings of the molecular structures for OCO-CN (upper) and COO-OCH_3 (lower) along with the numbering schemes. Two benzene rings in a biphenyl moiety are approximately coplanar, having dihedral angles of 3.4(7)° (OCO-CN) and 11.3(5)° (COO-OCH_3). In each crystal, the carbonyloxy plane is approximately coplanar with the benzene ring to which the C atom of the carbonyloxy group is attached, having dihedral angles of 3.8(11)° (OCO-CN) and 5.5(7)° (COO-OCH_3). Paraffin chains have all-*trans* conformations in both crystals, and the planes of the C–C–C backbones are slightly twisted with the biphenyl moieties, having dihedral angles of 12.9(15)° (OCO-CN) and 15.1(10)° (COO-OCH_3).

Table 1. Experimental Datails, Crystal Data and Final Results of Refinements

	OCO-CN	COO-OCH_3
Formula	$C_{28}H_{29}NO_3$	$C_{28}H_{32}O_4$
FW	427.52	432.54
Cryst. shape	Plate	Plate
Cryst. size/mm	0.3×0.4×0.05	0.5×0.4×0.05
l.s. for cell const.		
No. of refl.	19	20
2θ range/°	37—52	38—48
Space group	$Pca2_1$	$Pca2_1$
a/Å	7.41(3)	7.41(5)
b/Å	52.10(3)	53.21(3)
c/Å	6.10(3)	6.07(4)
V/Å^3	2353(14)	2393(23)
Z	4	4
D_x/g cm^{-3}	1.207	1.200
μ/cm^{-1}	6.16	6.27
F(000)	912	928
*R*1[a]	0.0805	0.0886
*wR*2[b]	0.3037	0.5275
No. of unique refl.	1550	1915
No. of obsd refl. ($>4\sigma(F_o)$)	925	1630
$(\Delta/\sigma)_{max}$	0.001	0.043
$\Delta\rho$/e Å^{-3}	0.261, −0.278	0.256, −0.364

a) $R1 = \Sigma||F_o| - |F_c||/\Sigma|F_o|$ for obsd reflections. b) $wR2 = [\Sigma w(F_o^2 - F_c^2)^2/\Sigma w(F_o^2)^2]^{0.5}$ for all reflections, where $w = 1/[\sigma^2(F_o^2) + (0.1575P)^2 + 2.1050P]$ where $P = (F_o^2 + 2F_c^2)/3$ for OCO-CN, and $w = 1/[\sigma^2(F_o^2) + (0.1982P)^2 + 1.6749P]$ where $P = (F_o^2 + 2F_c^2)/3$ for COO-OCH_3.

Table 2. Atomic Coordinates with Their Estimated Standard Deviations in Parentheses and Equivalent Isotropic Displacement Parameters for OCO-CN

Atom	*x*	*y*	*z*	*U*(eq)[a]/Å^2
O(1)	0.8788(13)	0.3776(2)	0.143(2)	0.089(3)
O(2)	1.0154(11)	0.3573(1)	0.4251(17)	0.067(3)
O(3)	0.9801(12)	0.1815(1)	−0.1661(17)	0.072(3)
N(1)	1.0947(19)	0.4882(2)	0.911(3)	0.118(6)
C(1)	1.068(2)	0.4706(2)	0.815(3)	0.084(5)
C(2)	1.0328(18)	0.4476(2)	0.686(3)	0.067(4)
C(3)	1.0848(17)	0.4240(2)	0.778(2)	0.068(4)
C(4)	1.0507(17)	0.4015(2)	0.658(3)	0.069(4)
C(5)	0.9786(17)	0.4024(2)	0.449(3)	0.061(4)
C(6)	0.9271(16)	0.4257(2)	0.360(2)	0.067(4)
C(7)	0.956(2)	0.4481(2)	0.477(3)	0.081(5)
C(8)	0.9503(18)	0.3784(2)	0.323(3)	0.064(4)
C(9)	1.0029(17)	0.3337(2)	0.325(3)	0.056(3)
C(10)	0.9220(17)	0.3146(2)	0.437(3)	0.069(4)
C(11)	0.9239(18)	0.2897(2)	0.355(2)	0.068(4)
C(12)	0.9996(16)	0.2833(2)	0.163(3)	0.055(4)
C(13)	1.0779(17)	0.3038(2)	0.047(3)	0.071(4)
C(14)	1.0814(17)	0.3282(2)	0.133(3)	0.071(4)
C(15)	0.9977(16)	0.2572(2)	0.075(3)	0.053(3)
C(16)	0.9103(16)	0.2367(2)	0.176(3)	0.063(4)
C(17)	0.9080(17)	0.2125(2)	0.098(3)	0.065(4)
C(18)	0.9957(16)	0.2063(2)	−0.096(3)	0.057(4)
C(19)	1.0862(16)	0.2256(2)	−0.212(3)	0.064(4)
C(20)	1.0859(15)	0.2505(2)	−0.121(3)	0.067(4)
C(21)	1.0445(18)	0.1742(2)	−0.375(3)	0.074(4)
C(22)	0.9674(17)	0.1487(2)	−0.423(3)	0.083(5)
C(23)	1.0380(18)	0.1362(2)	−0.634(3)	0.081(5)
C(24)	0.9634(18)	0.1095(2)	−0.679(3)	0.082(5)
C(25)	1.041(2)	0.0957(2)	−0.870(4)	0.096(5)
C(26)	0.965(2)	0.0684(2)	−0.896(5)	0.114(7)
C(27)	1.051(3)	0.0542(3)	−1.082(4)	0.133(8)
C(28)	0.981(3)	0.0273(3)	−1.120(5)	0.192(12)

a) *U*(eq) is defined as one third of the trace of the orthogonalized U_{ij} tensor.

Crystal Packings. Both crystals have very similar packing modes, as shown in Fig. 2 (OCO-CN) and Fig. 3 (COO-OCH_3) viewed along the *a* axis. They have smectic-like structures comprising bilayers stacked along the *b* axis. In a layer, alkyl chains and core moieties (except for the chains) aggregate separately with the tilt angle of the core moiety being about 20°. The nearest phenyl rings between adjacent molecules make angles of about 50° (OCO-CN) and about 65° (COO-OCH_3), resulting in a 'herring-bone' structure. Alkyl chains are closely arranged as in long-chain compounds. Figure 4 shows the intermolecular distances in the crystal structures of OCO-CN (left) and COO-OCH_3 (right). The C=O bonds form one-dimensional head-to-tail arrangements along the *c* axis, while they point up and down alternatively along the *a* axis, resulting in polar structures

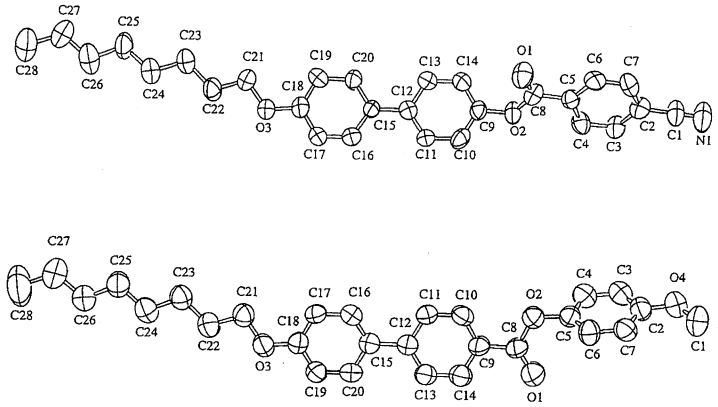

Fig. 1. The molecular structures of OCO-CN (upper) and COO-OCH_3 (lower) shown with 50% probability thermal ellipsoids. H atoms have been omitted for clarity.

Table 3. Atomic Coordinates with Their Estimated Standard Deviations in Parentheses and Equivalent Isotropic Displacement Parameters for COO-OCH_3

Atom	x	y	z	U(eq)[a]/Å^2
O(1)	0.6207(10)	0.3550(1)	0.8879(14)	0.115(3)
O(2)	0.4768(7)	0.3691(1)	0.5859(12)	0.084(2)
O(3)	0.5188(7)	0.1774(1)	0.1068(12)	0.084(2)
O(4)	0.5185(9)	0.4690(1)	0.8269(15)	0.103(2)
C(1)	0.4347(17)	0.4782(2)	1.019(3)	0.139(5)
C(2)	0.5022(11)	0.4439(1)	0.776(2)	0.084(3)
C(3)	0.5871(11)	0.4357(2)	0.5940(19)	0.091(3)
C(4)	0.5827(11)	0.4107(1)	0.5252(19)	0.089(2)
C(5)	0.4926(10)	0.3941(1)	0.6602(16)	0.076(2)
C(6)	0.4092(11)	0.4018(1)	0.8454(19)	0.086(3)
C(7)	0.4144(11)	0.4268(1)	0.9127(18)	0.086(2)
C(8)	0.5445(10)	0.3506(2)	0.7149(17)	0.078(2)
C(9)	0.5253(9)	0.3254(1)	0.6199(15)	0.071(2)
C(10)	0.4517(11)	0.3214(1)	0.4154(17)	0.080(2)
C(11)	0.4372(10)	0.2971(1)	0.3302(16)	0.075(2)
C(12)	0.5009(9)	0.2764(1)	0.4519(15)	0.068(2)
C(13)	0.5682(10)	0.2812(1)	0.6592(15)	0.077(2)
C(14)	0.5810(10)	0.3051(1)	0.7426(18)	0.083(2)
C(15)	0.4993(9)	0.2506(1)	0.3547(16)	0.068(2)
C(16)	0.4090(9)	0.2448(1)	0.1656(14)	0.074(2)
C(17)	0.4102(9)	0.2206(1)	0.0727(14)	0.072(2)
C(18)	0.5021(9)	0.2016(1)	0.1804(14)	0.070(2)
C(19)	0.5915(10)	0.2071(1)	0.3738(14)	0.076(2)
C(20)	0.5893(10)	0.2307(1)	0.4591(14)	0.074(2)
C(21)	0.4514(12)	0.1711(1)	−0.1062(17)	0.084(2)
C(22)	0.5311(11)	0.1457(1)	−0.1576(19)	0.091(3)
C(23)	0.4590(12)	0.1335(1)	−0.3704(19)	0.090(3)
C(24)	0.5371(12)	0.1074(1)	−0.402(2)	0.097(3)
C(25)	0.4593(14)	0.0940(2)	−0.604(2)	0.103(3)
C(26)	0.5337(15)	0.0674(2)	−0.628(2)	0.112(4)
C(27)	0.4514(19)	0.0534(2)	−0.822(3)	0.152(5)
C(28)	0.515(2)	0.0270(2)	−0.849(4)	0.234(12)

a) U(eq) is defined as one third of the trace of the orthogonalized U_{ij} tensor.

along the c axis. The distances between O1 (x, y, z) and C8 (x', y', z') are 3.13(2) Å (OCO-CN, x', y', $z'=1.5-x$, y, $-0.5+z$) and 3.19(2) Å (COO-OCH_3, x', y', $z'=1.5-x$, y, $0.5+z$), which are comparable to the expected value for

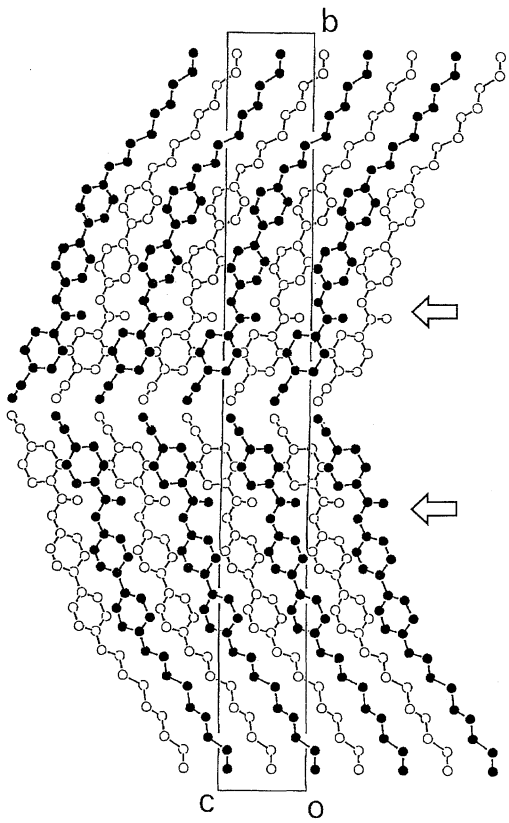

Fig. 2. The crystal structure of OCO-CN viewed along the a axis. Atoms of front molecules are shown by solid circles and those of behind ones are shown by open circles. Arrows denote the directions of accumulated dipole moments.

van der Waals contact, 3.2 Å. The directions of the accumulated dipole moments are opposite with respect to the tilt of the molecular long axes between the two crystals, as shown by the arrows in Figs. 2 and 3. The interatomic distances, 3.96(3) Å for C1 (x, y, z) and C1 ($1-x$, $1-y$, $0.5+z$) and 3.40(2) Å for C1 (x, y, z) and O4 ($1-x$, $1-y$, $0.5+z$), indicate a van der Waals contact of the two methoxy groups between layers (2.0 Å for methyl and 1.52 Å for oxygen). On the other hand, in OCO-CN, negatively polarized N atoms of strong CN dipoles face each other, suggesting an unfa-

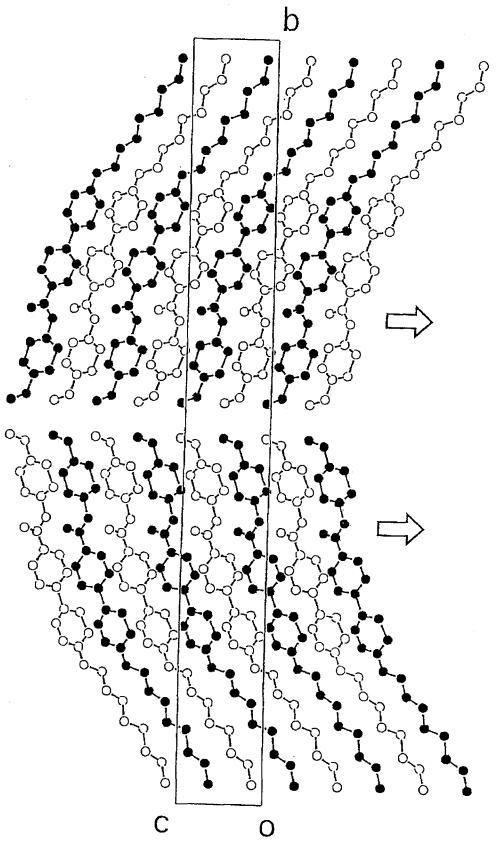

Fig. 3. The crystal structure of COO-OCH_3 viewed along the a axis. Atoms of front molecules are shown by solid circles and those of behind ones are shown by open circles. Arrows denote the directions of accumulated dipole moments.

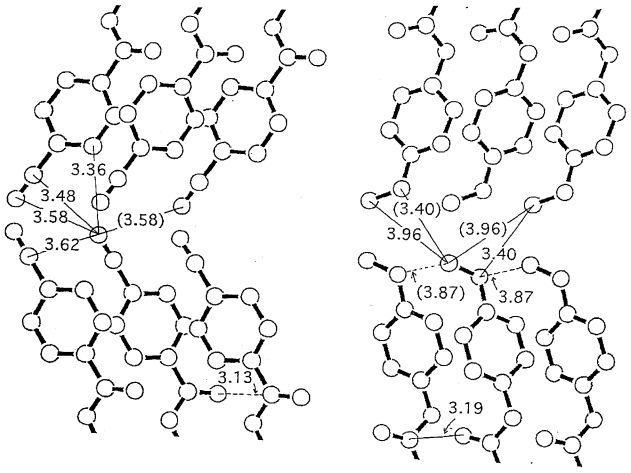

Fig. 4. Intermolecular distances (in Å) in the crystal structures of OCO-CN (left) and COO-OCH_3 (right), shorter than 3.8 and 4.0 Å, respectively. Solid and broken lines denote connections of atoms from the central molecule to the upper and lower molecules along the a axis, respectively. Symmetry-related values are denoted in parentheses.

vorable arrangement for crystal packing. This feature is in contrast to those of many other mesogenic compounds bearing terminal CN groups. For them, more or less attractive arrangements have been found: e.g., antiparallel arrangements of CN groups (C···N distances, 3.39—3.63 Å)[5,14—16] and close arrangements between CN and ester linkage (N···C in COO, 3.39—3.59 Å)[5] and between CN and phenyl ring (N···C in phenyl, 3.39 Å).[16] The distance of N (x, y, z) and N ($2-x$, $1-y$, $0.5+z$) between cyano groups in the crystal of OCO-CN is 3.58(2) Å, significantly longer than that expected for van der Waals contact, 3.1 Å, which would reduce the repulsive forces.

Crystal to Mesophase Transition Behavior. It was reported that the crystal of OCO-CN at room temperature transforms to a higher-temperature crystalline phase, and then to the S_{A1} phase, by DSC measurements.[3] It is remarkable that the peak of the crystal-to-crystal phase transition was relatively high. To certify the thermodynamic states of the present crystals, the structures of which have been determined, we also carried out DSC measurements for single crystals of both compounds. Figure 5 shows DSC traces of the crystals of OCO-CN and COO-OCH_3. OCO-CN showed the same behavior as was reported: the cystal–crystal (peak a) and crystal-S_A (peak b) phase transitions at 97 °C and 127 °C, respectively. COO-OCH_3 also showed an endothermic peak c (91 °C) attributable to a cystal–crystal transition below the melting peak d (114 °C). Thus, we denote the present single crystals as CR1, which transform to higher temperature crystals, CR2; i.e., the phase sequence is CR1–CR2–S_A–N–iso. for both compounds.

The ΔS value of the CR1–CR2 transition (45±3 $J\,K^{-1}\,mol^{-1}$) is comparable to that of the CR2–S_A transition (49±4 $J\,K^{-1}\,mol^{-1}$) for OCO–CN, while that of the CR2–S_A transition (82±5 $J\,K^{-1}\,mol^{-1}$) is four-times as large as that of the CR1–CR2 transition (18±2 $J\,K^{-1}\,mol^{-1}$) for COO-OCH_3. Therefore, the CR2 of OCO-CN is much more disordered than that of COO-OCH_3. However, the total ΔS values from CR1 to S_A are almost equal, 95±7 and 100±7 $J\,K^{-1}\,mol^{-1}$ for OCO-CN and COO-OCH_3, respectively. Since the structures of CR1 for OCO-CN and COO-OCH_3 resemble each other, similar S values are expected for both crystals, and hence for the S_A phases of OCO-CN and COO-OCH_3.

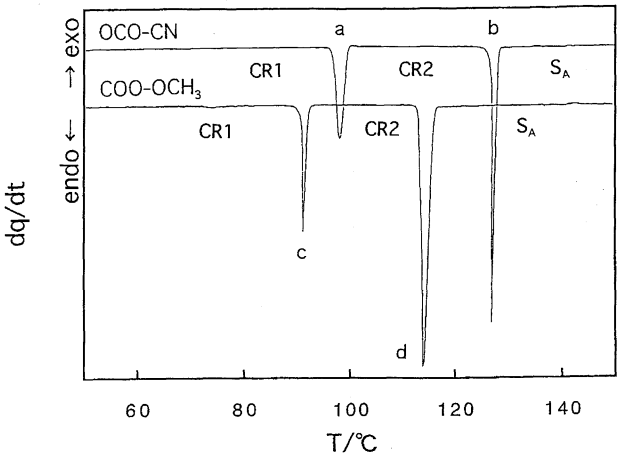

Fig. 5. DSC traces on heating with the heating rate of 1 $K\,min^{-1}$ for the crystals of OCO-CN and COO-OCH_3.

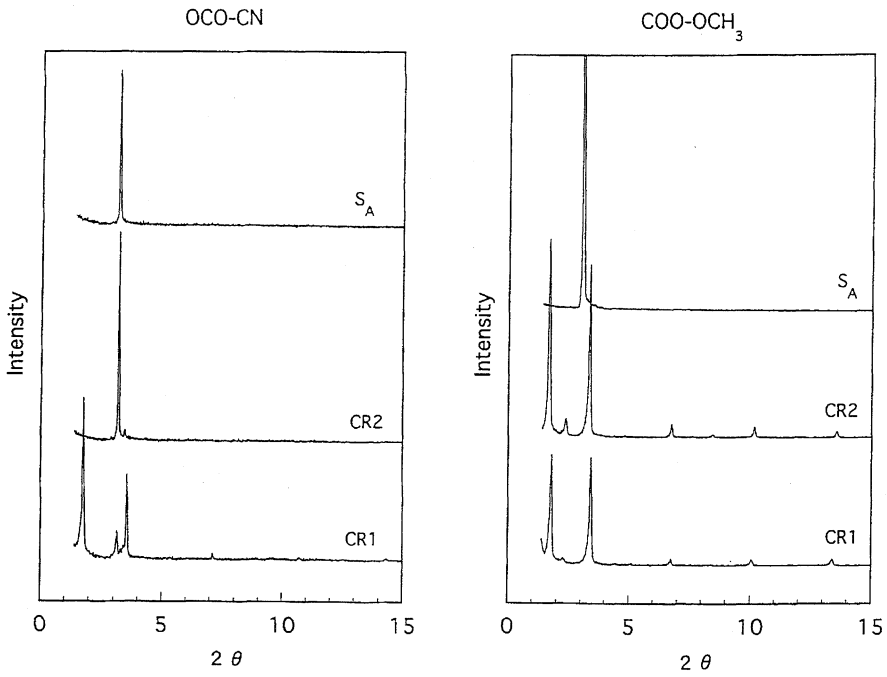

Fig. 6. Powder X-ray diffraction patterns of OCO-CN (left) and COO-OCH_3 (right) at S_A, CR2, and CR1. (130 °C, 120 °C, and 25 °C for OCO-CN and 140 °C, 110 °C, and 25 °C for COO-OCH_3).

In order to elucidate structural changes during the phase transition, CR1–CR2–S_A, powder X-ray diffraction patterns were obtained. As shown in Fig. 6, each compound shows peaks at about 50 Å (at 2θ=1.7°) and 25 Å (at 2θ=3.5°), corresponding to the 010 and 020 reflections, respectively, for CR1 and only one peak at 27 Å (at 2θ=3.2° for OCO-CN) or 28 Å (at 2θ=3.1° for COO-OCH_3) for the S_A phase. On the other hand, the structures of CR2 were found to be different. For COO-OCH_3, the peak at 50 Å still exist, showing that a bilayer structure is maintained. On the other hand, at the transition of CR1–CR2 of OCO–CN, the peak at 50 Å disappears and peaks at 25 and 28 Å appear. The latter becomes dominant in intensity upon heating. Higher order reflections vanish, indicating that the stacking of layers is not crystalline, but very disordered with a periodicity of one molecular length. Thus, it is concluded that CR2 of OCO-CN is a monolayer structure, while CR2 of COO-OCH_3 still has a bilayer structure. These facts are consistent with the DSC results. As mentioned above, the ΔS values of the CR1–CR2 transition are 50% (OCO-CN) and 20% (COO-OCH_3) of the total amount of the CR1–CR2–S_A transitions; i.e., at the CR1–CR2 transition for OCO-CN the structural change from the periodicity of two molecular length to one molecular length is much greater. Here, a question may arise. Why are the structures of CR2 different, although they are sandwiched between almost the same CR1 and S_A structures? One possible interpretation is as follows. When the intermolecular interaction becomes weak as the temperature increases, the bilayer structure of OCO-CN would become unstable due to the unfavorable arrangement of the CN groups mentioned above. On the other hand, in the case of COO-OCH_3, the polarizable methoxy group would maintain the bilayer structure, until the thermal agitation overcomes the interlayer interaction at higher temperature.

Conclusions

It is concluded that the combination of two factors, (1) the opposite properties of the terminal polar groups (electron-donating or -accepting) and (2) the opposite directions of the central ester linkages, results in almost the same crystal packing of molecules for OCO-CN and COO-OCH_3. Here, distinct smectic-like layer structures with a small tilt angle (20°) are closely related to the phase sequence of crystal–S_A–N-iso. for them. In the crystal of OCO-CN, any specific interaction responsible for the dimer formation, which was found for many other cyano compounds, is not found around the CN groups, being closely related to the S_A phase comprising monolayers. Different high-temperature crystalline phases (CR2), a monolayer structure for OCO-CN and a bilayer one for COO-OCH_3, appear between the room-temperature crystalline (CR1) and S_A phases, with almost the same amount of total entropy gain throughout the transition process, CR1–CR2–S_{A1}.

We thank Dr. Yoichi Takanishi of Tokyo Institute of Technology for his help in the measurements of powder X-ray diffraction patterns. This work was supported by a Grant-in-Aid for Scientific Research No. 08640638 from the Ministry of Education, Science, Sports and Culture.

References

1) J. W. Goodby, T. M. Leslie, P. E. Cladis, and P. L. Finn, "Liquid Crystals and Ordered Fluids," ed by A. C. Griffin and J. F. Johnson, Plenum Press, New York (1984), Vol. 4, p. 89; P. E. Cladis, P. L. Finn, and J. W. Goodby, "Liquid Crystals and Ordered

Fluid," Plenum Press, New York (1984), Vol. 4, p. 203.

2) H. Takeda, Y. Sakurai, S. Takenaka, H. Miyake, T. Doi, and S. Kusabayashi, *J. Chem. Soc., Faraday Trans.*, **86**, 3429 (1990).

3) J. W. Goodby and C. R. Walton, *Mol. Cryst. Liq. Cryst.*, **122**, 219 (1985).

4) A. J. Leadbetter, R. M. Richardson, and C. N. Colling, *J. Phys.* (*Orsay, Fr.*), **36**, Cl-37 (1975).

5) F. Hardouin, A. M. Levelut, and G. Sigaud, *J. Phys.* (*Orsay, Fr.*), **42**, 71 (1981).

6) H. Iki and K. Hori, *Bull. Chem. Soc. Jpn.*, **68**, 1281 (1995).

7) K. Hori and Y. Nishiura, *Acta Crystallogr., Sect. C*, **C52**, 2922 (1996).

8) G. J. Gilmore, "MITHRIL84. A Program for the Solution of the Crystal Structures," (1984).

9) G. M. Sheldrick, "SHELXS86. A Program for the Solution of the Crystal Structures," University of Göttingen (1986).

10) G. M. Sheldrick, "SHELXL93. Program for the Refinement of the Crystal Structure," University of Göttingen (1993).

11) A. J. C. Wilson, "International Tables for Crystallography," Kluwer Academic Publishers, Dordrecht (1993), Vol. C.

12) Lists of structure factors, anisotropic temperature factors for non-hydrogen atoms, atomic parameters for H atoms, and bond lengths and angles have been deposited as Document No. 71012 at the Office of the Editor of Bull. Chem. Soc. Jpn.

13) C. K. Johnson, "ORTEPII, Report ORNL-5138," Oak Ridge National Laboratory, Tennessee, USA (1976).

14) K. Hori, Y. Koma, A. Uchida, and Y. Ohashi, *Mol. Cryst. Liq. Cryst.*, **225**, 15 (1993).

15) K. Hori, Y. Koma, M. Kurosaki, K. Itoh, H. Uekusa, Y. Takenaka, and Y. Ohashi, *Bull. Chem. Soc. Jpn.*, **69**, 891 (1996).

16) K. Hori, M. Kurosaki, H. Wu, and K. Itoh, *Acta Crystallogr., Sect. C*, **C52**, 1751 (1996).